High brightness AlGaInP-based light emitting diodes by adopting the stripe-patterned omni-directional reflector

2006 Semicond. Sci. Technol. 21 184

(http://iopscience.iop.org/0268-1242/21/2/016)

INSTITUTE OF PHYSICS PUBLISHING SEMICONDUCTOR SCIENCE AND TECHNOLOGY

Semicond. Sci. Technol. **21** (2006) 184–189 doi:10.1088/0268-1242/21/2/016

High brightness AlGaInP-based light emitting diodes by adopting the stripe-patterned omni-directional reflector

Y J Lee[1,2], T C Lu[1], H C Kuo[1], S C Wang[1], M J Liou[2], C W Chang[2], T C Hsu[2], M H Hsieh[2], M J Jou[2] and B J Lee[2]

[1] Department of Photonic and Institute of Electro-Optical Engineering, National Chiao Tung University, 1001 Ta Hsueh Road, Hinchu 300, Taiwan, Republic of China

[2] R&D Division, Epistar Co., Ltd, Science-based Industrial Park, Hsinchu 300, Taiwan, Republic of China

Received 19 October 2005, in final form 7 December 2005
Published 12 January 2006
Online at stacks.iop.org/SST/21/184

Abstract

An n-side-up AlGaInP-based LED operating at a wavelength of 630 nm with a stripe-patterned omni-directional reflector (ODR) was fabricated by adopting the adhesive-layer bonding scheme. It is demonstrated that the periodic and geometrical shape of the stripe-patterned array improves the light extraction efficiency by increasing the extraction of guided light. Compared to the conventional ODR LED, the stripe-patterned ODR LED significantly enhanced the output power and with only a slightly higher forward voltage. This improvement was analysed by the scanning near-field optical microscope (SNOM) and the optimized dimension of stripe patterns was also calculated on the basis of a Monte Carlo ray tracing simulation. According to the above analysis, the increase of light extraction could not only be attributed to the geometrical shape of the stripe patterns that redirect the trapped light towards the top-escaping cone of the LED surface but also to the repetitive stripe-patterned array of diffracting elements that effectively diffract the guided light outside the LED surface. Moreover, the optimized dimension of the stripe pattern is 3 μm wide, 2 μm deep and spaced 3 μm apart, which coincides with experimental results.

(Some figures in this article are in colour only in the electronic version)

Introduction

For the yellow-to-red spectral region, the quaternary AlGaInP material system, grown by low-pressure metal-organic chemical vapour deposition (MOCVD), has proven to be the best choice in many applications such as interior and exterior automotive lighting, traffic lights, full colour displays, and all kinds of indoor and outdoor signs [1, 2]. A new level of high light efficiency was achieved over this spectral regime. Due to the intense investigation of previous studies, the epitaxial technology of AlGaInP materials was quite mature, and as a consequence, around 100% internal quantum efficiency was achieved [3]. However, the quaternary AlGaInP LEDs suffer poor light extraction efficiency due to the total internal reflection of light between air (epoxy) and the semiconductor. Approximately $1/(4n^2)$ of the light from the active region can escape from the top and bottom of the device, where n denotes the refractive index of semiconductor materials [4]. Furthermore, the AlGaInP LEDs are grown on GaAs substrates that are opaque for the emitting wavelengths of this quaternary material. Hence, most of the light radiated from the active region is trapped in the device and is eventually absorbed by the GaAs absorbing substrate. Thus, the major issue was then how to get the photons that had been generated

inside the active region out from the semiconductor LEDs to where they could be used. There are many approaches to enhance the photon escape probability of AlGaInP-based LEDs. The first hurdle was to prevent light from being absorbed by the GaAs substrate. One common method is the insertion of a distributed Bragg reflector (DBR) sandwiched between the absorbing GaAs substrate and LED structure [5, 6]. However, only the radiated light impinging near normal to the DBR can be effectively reflected. As for the oblique angles of radiated light, the DBR becomes transparent and the light is subsequently absorbed by the GaAs substrate. Another successful technique is removal of the GaAs substrate by etching and replacement with GaP transparent substrate (TS) by wafer bonding [7–9]. However, the process is costly and complicated. Recently, a thin-film technique combined with a wafer bonding scheme and omni-directional reflector (ODR) has been presented as a novel approach to improve the light extraction efficiency [10–12]. This design allows radiated light with any incident angle to be reflected from the ODR to the top surface of the device. Also it offers a cost advantage over the TS technique. Although the light radiated towards the substrate direction with any incident angle can be more effectively reflected on the top surface of the device with an ODR, the light that can escape from the LED structure is still small due to the large step change in the index of refraction at the interface between the AlGaInP material and the air. To overcome the above issue, Illek *et al* proposed a buried micro-reflector (BMRs) structure for boosting the AlGaInP LED performance [13]. In our previous work, we also observed that the light output of LEDs was improved by specifically controlling the geometric shape of stripe patterns through inductively coupled plasma (ICP) etching [14]. In this study, we report on AlGaInP-based LEDs with integrated stripe-patterned omni-directional reflector to enhance the light extraction and the dimensions of the stripe-patterned ODR are also optimized by the Monte Carlo ray tracing simulation.

Device fabrication

A schematic cross-section image of an ODR quaternary AlGaInP LED combing with the stripe-pattern structure is shown in figure 1(*a*). The LEDs employed in this paper were grown by low-pressure metal-organic chemical vapour deposition (Aixtron 2600G) on a nominal (1 0 0) plane 15° off towards the [1 1 1] direction n^+-GaAs substrate. The LED structure consisted of a 0.6 μm Si-doped n-$Al_{0.5}In_{0.5}P$ cladding layer, a multiple quantum well (MQW) active layer region, a 0.5 μm Mg-doped p-$Al_{0.5}In_{0.5}P$ cladding layer, a 5 μm Mg-doped p-GaP window layer and a 50 nm Mg-doped p^+-GaP ohmic contact layer. The MQW active layer of the AlGaInP-based LED consisted of 24 undoped $In_{0.5}Ga_{0.5}P$ well layers separated by 25 Si-doped $(Al_{0.3}Ga_{0.7})_{0.5}In_{0.5}P$ barrier layers. The peak wavelength of this AlGaInP LED was 630 nm. The stripe pattern was defined on the GaP layer by standard photolithography with the dimensions of 3 μm width, 2 μm depth and a period of 6 μm. Next, an inductively coupled plasma (ICP) dry-etching system with etching gas of BCl_3–HBr was used to form the GaP stripe patterns (figure 1(*b*)). This was followed by a calculated

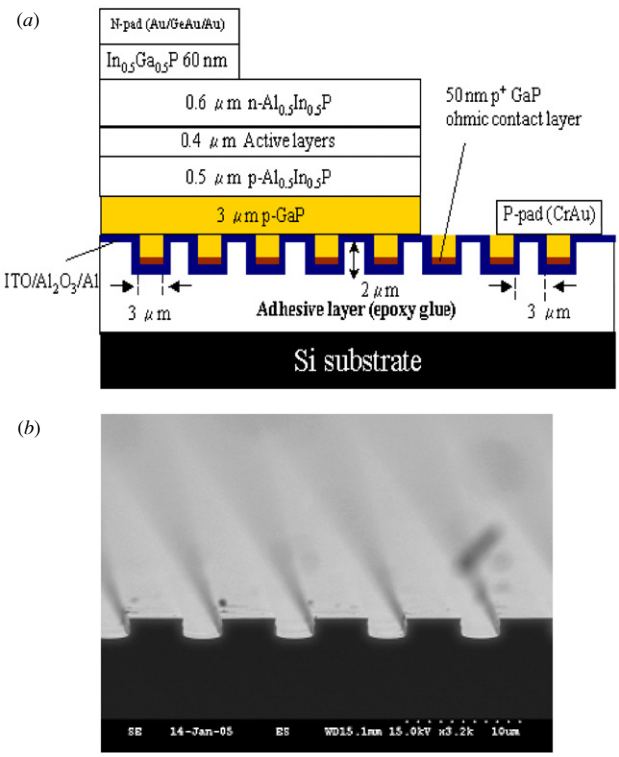

Figure 1. (*a*) A schematic of the AlGaInP stripe-patterned LED, and (*b*) cross-sectional SEM micrograph of the stripe-patterned ODR after ICP dry etching.

reflection of about 90% ODR mirror system composed of a 100 nm ITO current spreading layer, a 100 nm Al_2O_3 low index layer and a 300 nm Al metal layer, deposited layer by layer on the surface of the stripe-patterned GaP by e-beam evaporation. The p-side of the LED structure and the Si substrate carrier were then brought into contact with the commercially available epoxy glue bonding at the operating temperature of 80 °C. The n-type GaAs substrate was subsequently removed by using a NH_4OH-based solution and, then, the etching was stopped on the 60 nm Si-doped n-$In_{0.5}Ga_{0.5}P$ ohmic contact layer. The emitting area was then defined by ICP dry etching until the exposure of the ITO current spreading layer. Finally, Au/GeAu/Au and Cr/Au were deposited as n and p electrodes, respectively. Thus, current injected from the p electrode effectively spreads through the ITO current spreading layer into the ridge regions of the GaP layer because only these ridge regions contain highly doped layer (50 nm Mg-doped p^+-GaP layer) and that makes ohmic contact with the ITO current spreading layer. The wafer was then cut into 350 μm × 350 μm chips. Typical ODR LEDs with exactly the same process procedure except without the stripe pattern were prepared for comparison. These chips were n-side-up mounted on a lead frame and moulded in epoxy resin for the subsequent measurement. Typical current–voltage (*I–V*) measurements were performed using a high current measuring unit (Keithley 240). The light output power of the LEDs was measured using an integrated sphere with a calibrated power meter.

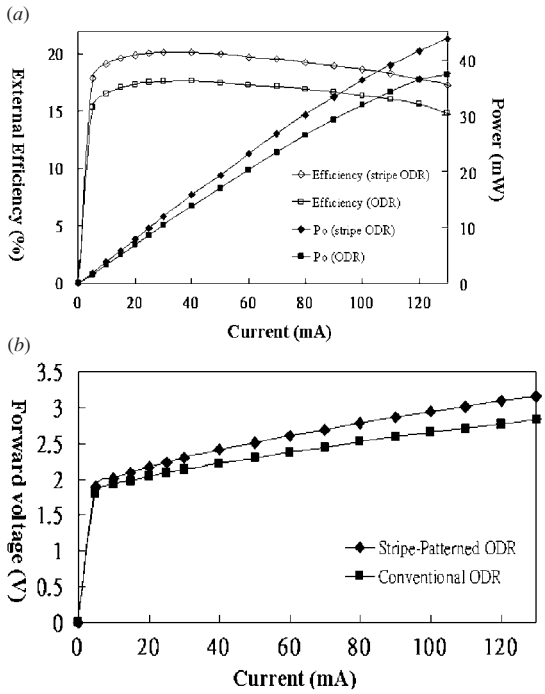

Figure 2. (*a*) The output power (*L–I* curve) and external quantum efficiency, and (*b*) the current–voltage (*I–V*) characteristics of conventional and stripe-patterned ODR LEDs as a function of the forward-bias current.

Results and discussion

Figure 2(*a*) shows the measurement results of room temperature output power (*L–I* curve) and external quantum efficiency of conventional and strip-patterned ODR LEDs as a function of the forward-bias current. The *L–I* curves of both devices show the linear features under our measurement condition of the driving current up to 130 mA. Due to the higher thermal conductivity of Si compared to that of the GaAs substrate, these devices are advantageous for high power operation. The light output powers at 20 mA of the conventional and stripe-patterned ODR LEDs are 6.8 and 7.8 mW, respectively. In comparison with the output power for conventional and stripe-patterned ODR LEDs, these GaP stripe patterns improved the light output power by an approximate factor of 1.15. The external quantum efficiency of both structures has the same tendency with the driving current, indicating near the same internal quantum efficiency due to exactly the same epitaxial structure and quality. Even though the external efficiency of the stripe-patterned ODR LED in absolute terms does not exceed state-of-the-art devices using other approaches, comparison is being made on the overall output power enhancement adopting the geometrical shape of stripe patterns. Figure 2(*b*) shows the current–voltage (*I–V*) characteristics of conventional and strip-patterned ODR LEDs. The larger forward voltage of the stripe-patterned ODR LED compared to the conventional ODR LED was observed in this figure up to 130 mA. For the stripe-patterned ODR LED, about half of the highly doped layer (50 nm Mg-doped p^+-GaP layer) area that makes contact with the ITO current spreading layer is etched away to form the stripe pattern, which reduces the p-ohmic contact region and finally increases the contact

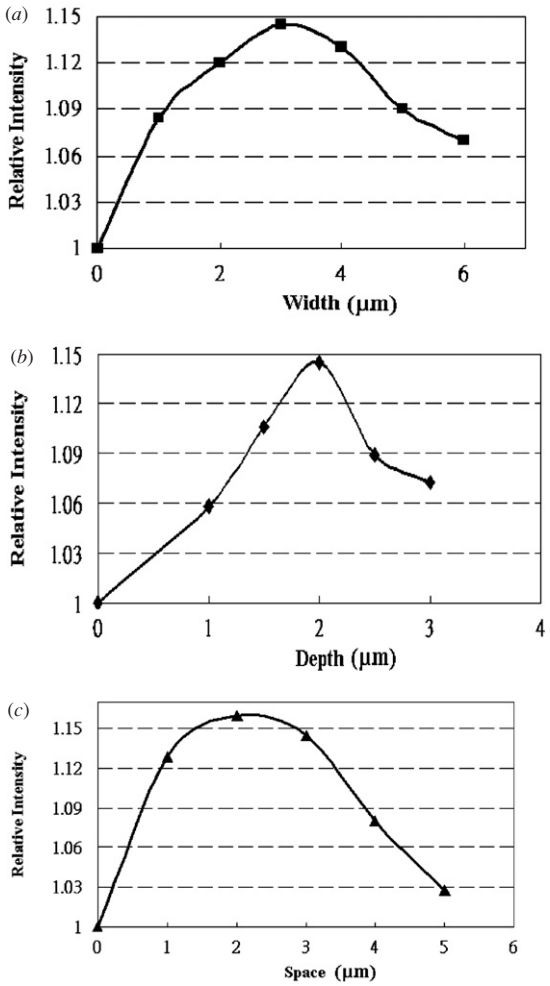

Figure 3. The calculated enhancement of stripe-patterned ODR LEDs relative to the conventional ODR LEDs as a function of stripe (*a*) width, (*b*) depth and (*c*) spacing.

resistance. In order to investigate the enhancement tendency of light extraction efficiency with different dimensions of stripe patterns, standard and commercially available Monte Carlo ray tracing software was used with a simple and straightforward model. Figure 3(*a*) shows the calculated enhancement of stripe-patterned ODR LEDs relative to the conventional (flat) ODR LEDs as a function of stripe width, and the stripe depth and space are fixed at 2 μm and 3 μm, respectively. According to this figure, an optimized stripe width of 3 μm was obtained, and an approximately 15% enhancement compared to the flat ODR LED was observed, coinciding with our experimental measurement with this dimension of stripe pattern design. Fixing stripe width and spacing as 3 μm, the relative enhancement as a function of the stripe depth is depicted in figure 3(*b*). On the basis of this figure, the maximum enhancement was observed for the stripe patterns with an etching depth of 2 μm. Finally, the space between stripe patterns was also calculated, and the result is shown in figure 3(*c*). As can be seen in this figure, the optimized spacing of stripe patterns is roughly about 3 μm. This is also the reason why we choose the stripe patterns with the dimensions of 3 μm wide, 2 μm deep and a period of 6 μm to investigate in this study. The simulated far-field patterns of conventional and

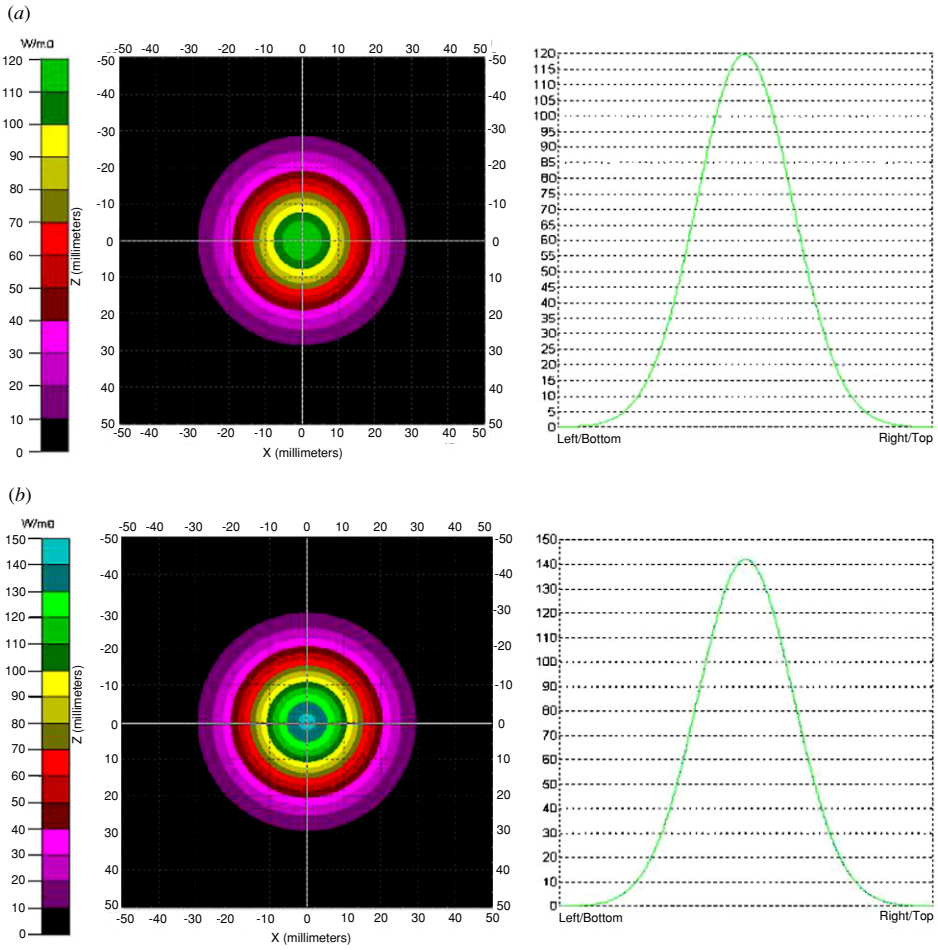

Figure 4. The simulated far-field patterns of (*a*) conventional and (*b*) stripe-patterned ODR LEDs. The cross section profile of intensity distribution is also shown in this figure.

stripe-patterned ODR LEDs are shown in figure 4. Stronger axial intensity on stripe-patterned ODR LEDs, about 1.15 times higher than that on conventional ODR LEDs, was observed in this figure, reiterating that the stripe-patterned ODR can effectively redirect the guided light to the top exit cone of the LED surface.

It is important to note that the Monte Carlo ray tracing simulation is based on the theory of geometrical optics, and the behaviour that is specifically attributable to the wave nature of light is not considered. However, with such micro-dimensions of stripe patterns, the physical optics should also be taken into account. The periodic stripe-patterned array can serve as a reflection diffraction grating. On reflection from this kind of grating, light scattered by the periodic stripe features will arrive at the LED surface with a definite phase relationship. The guided light supposed to be trapped inside the LED would be diffracted into different beams with orders that satisfy the constructive interference condition, adding the opportunity of the guided light to find the escaping cone. Figure 5 shows a simple optical ray diagram of the propagation of guided light as illustrated above.

To prove the geometric shape of the stripe pattern can improve light extraction, micro photoluminescence (micro-PL) of the stripe-patterned ODR LED has also been measured. Figure 6(*a*) shows the experimental set-up of the micro-PL

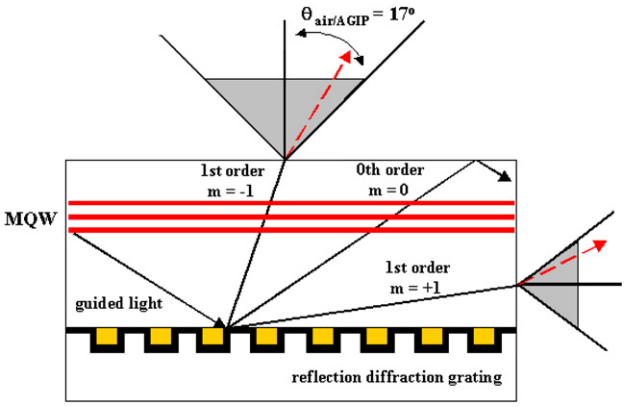

Figure 5. Simple optical ray diagrams in LEDs with the stripe-patterned array serving as the reflection diffraction grating.

system. The micro-PL system consists of a commercial microscope combined with a scanning near-field optical microscope (SNOM) and a confocal microscope. The stripe-patterned ODR LED sample was placed on a PZT-controlled stage with a resolution of 2 nm and excited with a 325 nm He–Cd laser through a 100× objective. The focused spot size on the sample was approximately 1 μm in diameter. By moving

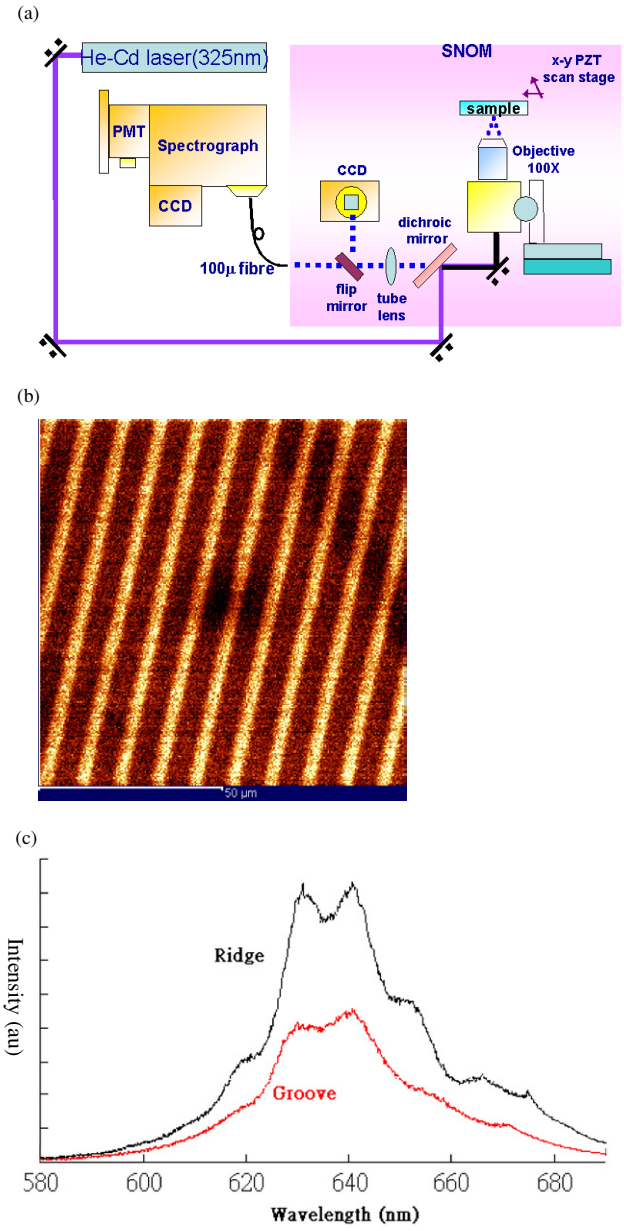

Figure 6. (*a*) The experimental set-up of micro-PL (μ-PL), (*b*) the μ-PL mapping image of the stripe-patterned ODR LED and (*c*) the μ-PL spectra obtained from the ridge region and groove region.

the PZT stage, the PL spectra of both the ridge and groove regions of the stripe pattern can be measured under the same excitation density and spot size. The PL emission from the sample was collected with the same 100× objective and fed to a 0.32 m spectrometer with a spectral resolution of 0.1 nm and a cooled UV-enhanced CCD. Figure 6(*b*) shows the micro-PL mapping image of the stripe-patterned ODR LED under a laser excitation intensity of approximately 30 kW cm^{-2}. In this figure, the integrated intensity of the ridge region is about 30% larger than that of the groove region, indicating that the stripe-patterned ODR LED really can increase the light extraction through its geometrical shape that redirects the guided light towards the top of the chip surface. The micro-PL spectra obtained from the ridge and groove regions are also shown in figure 6(*c*). The periodic fluctuation in the PL spectra

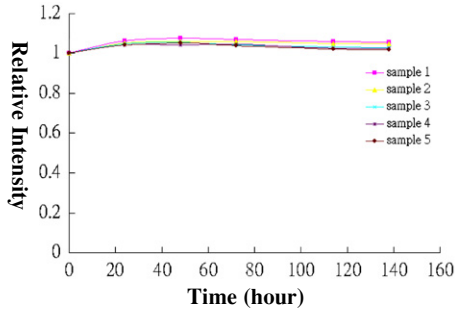

Figure 7. Reliability result of stripe-patterned LEDs under the stressed condition of 55 °C and drive current of 50 mA.

is caused by the Fabry–Perot interference between the ODR mirror system and air. In this figure, about twice the PL peak intensity was observed from the ridge region compared with that from the groove region, restating that the employment of the stripe-patterned structure is advantageous to the light extraction.

Figure 7 shows the degradation curves of the stripe-patterned ODR LED under the stress condition of 55 °C and at a drive current of 50 mA. No significant difference of ageing behaviour from the ODR LED exists. Good ageing behaviour was observed from this figure except for a small increase of light output during the first hours of stressed time, indicating the high light extraction efficiency by employing the stripe-patterned structure is a reliable and promising method for the device production.

Conclusion

High light-extraction-efficiency AlGaInP LEDs employing a stripe-patterned omni-directional reflector (ODR) were fabricated. Their optical and electrical characteristics were measured and compared to a non-patterned ODR LED. The output power of the stripe-patterned ODR LED at a driving current of 20 mA exceeds that of the typical ODR LEDs by a factor of 1.15, and with an acceptable forward voltage of about 2.2 V. According to the analysis using a scanning near-field optical microscope (SNOM), Monte Carlo ray tracing simulation and physical optics, the enhancement of the light extraction efficiency is not only attributable to the geometrical shape of the stripe-patterned ODR by redirecting the guided light towards the top-escaping cone of the LED surface but also to the repetitive stripe-patterned array of diffracting elements that effectively diffract the guided light outside the LED surface, adding the light extraction. The optimized dimensions of the stripe pattern are 3 μm width, 2 μm depth and 3 μm spacing. The stripe-patterned omni-directional reflector is expected to be a useful technique for realizing high brightness AlGaInP-based LEDs.

Acknowledgment

This work was supported in part by the National Science Council of Republic of China (ROC) in Taiwan under contract nos NSC 93-2120-M-009-006 and NSC 93-2752-E-009-008-PAE.

References

[1] Sugawara H, Ishikawa M and Hatakoshi G 1991 *Appl. Phys. Lett.* **58** 1010–12

[2] Kuo C P, Fletcher R, Osentowski T, Lardizabal M, Craford M and Robbins V 1990 *Appl. Phys. Lett.* **57** 2937–9

[3] Stringfellow G B and George Craford M 1997 *High Brightness Light Emitting Diodes* (Boston, MA: Academic)

[4] Boroditsky M and Yablonovitch E 1997 *Proc. SPIE* **3002** 119–22

[5] Sugawara H, Itaya K, Nozaki H and Hatakoshi G 1992 *Appl. Phys. Lett.* **61** 1775–7

[6] Chious S W, Lee C P, Huang C K and Chen C W 2000 *J. Appl. Phys.* **87** 2052–4

[7] Kish F A *et al* 1994 *Appl. Phys. Lett.* **64** 2839

[8] Höfler G E, Vanderwater D A, DeFevere D C, Kish F A, Camras M D, Steranka F M and Tan I-H 1996 *Appl. Phys. Lett.* **69** 803

[9] Krames M R *et al* 1999 *Appl. Phys. Lett.* **75** 2365

[10] Lekner J 2000 *J. Opt. A: Pure Appl. Opt.* **2** 349

[11] Gessmann T, Schubert E F, Graff J W, Streubel K and Karnutsch C 2003 *IEEE Electron Device Lett.* **24** 683

[12] Gessmann T, Luo H, Xi J-Q, Streubel K P and Schubert E F 2004 *Proc. SPIE Int. Soc. Opt. Eng.* **5366** 53

[13] Illek S, Jacob Ul, Plössl A, Stauss P, Streubel K, Wegleiter W and Wirth R 2002 *Compound Semiconductors* (Jan)

[14] Lee Y J *et al* 2005 *Mater. Sci. Eng.* B **122** 184